Diabetic Complications Consortium

Application Title: Macrophage-Targeted Nanocarriers for Localized Treatment of Chronic Inflammation in Diabetic Wounds

Principal Investigator: Smith, Andrew

1. Project Accomplishments:

This Pilot and Feasibility Study focused on the development of targeted therapeutics for diabetic wound. Specifically the project developed dextran conjugates of anti-inflammatory drugs that target monocytes/macrophages (MΦs) within the wound. The project enabled (1) the analysis of cell targeting and biodistribution in mouse models of diabetic wounds, and (2) the analysis of novel targeted anti-inflammatory agents.

2. Specific Aims:

Specific Aim 1: Engineer nanocarrier size for local monocyte/MΦ targeting.

Results: Shown in **Fig. 1A**, 6 hr after injection in wounds, ~80% of cells retaining the polysaccharide dextran 70 were monocyte/MΦs, our target population based on multiplex flow cytometry using dye-labeled dextran 70. Only ~7% of cells were structural (*e.g.* fibroblast or endothelial; $CD45^-$). In *in vitro* studies, inflammatory MΦs (lipopolysaccharide (LPS)-treated) exhibited ~3-fold higher uptake of conjugates compared with anti-inflammatory MΦs (interleukin-4 (IL4)-treated) (**Fig. 2B**). Shown in **Fig. 2**, we analyzed the size dependence of biodistribution of radioisotopic conjugates (^{64}Cu-NOTA) of polysaccharide nanocarriers for selective retention in wounds, injecting subcutaneously into one wound (Wound 1) with a second wound not injected (Wound 2). Wound 2 allows the analysis of uptake based on inflammation if any conjugates are released into circulation. Dextran with molecular weight of 10 kDa (**Fig. 2a**), which is near 4 nm in hydrodynamic diameter, partially retained in wounds (Wound 1), with some transporting away to kidneys. There was substantial uptake in Wound 2 at 6 hr. Retention between 6 hr and 24 hr were similar for most tissues except for Wound 2, which exhibited significantly reduced dextran 10. For dextran with molecular weight of 70 kDa (**Fig. 2b**), which is near 12 nm in hydrodynamic diameter, more was retained in the injected wound (Wound 1), with little distribution in other tissues. Distributions were similar at 6 hr and 24 hr time points.

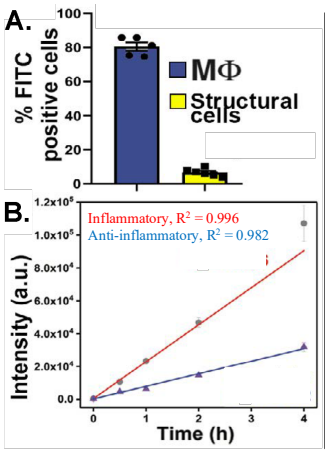

Fig. 1. Dextran-based nanocarriers associate with wound MΦs and are selectively taken up by inflammatory MΦs. (A) FITC-labeled dextran (70 kDa, 1 mg/mL) was subcutaneously injected into mouse wounds which underwent multiplex flow cytometry for FITC uptake in recruited monocyte/MΦs (live,$lin^-CD3^-CD19^-Ly6G^-CD11b^+$) compared to structural wound cells (live, $CD45^-$), 6 hr after injection. **(B)** *In vitro* time-dependent uptake of dextran by inflammatory (LPS) or anti-inflammatory (IL4) mouse MΦs.

Specific Aim 2: Evaluate wound closure and side effects after chronic dosing.

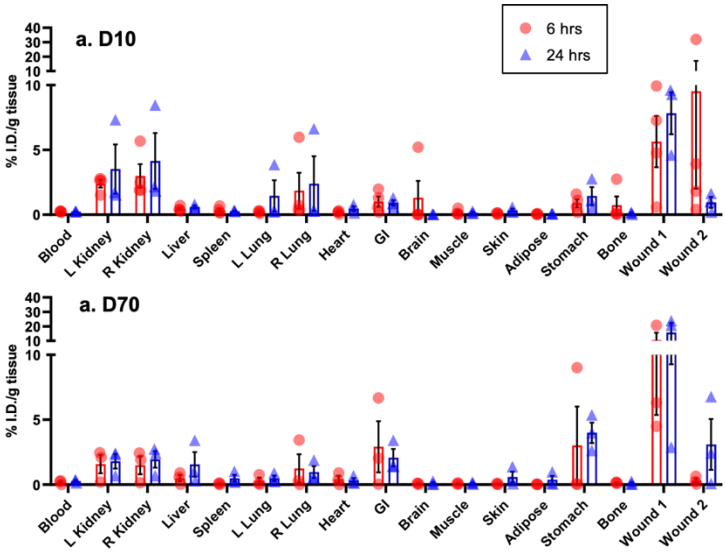

Fig. 2. ^{64}Cu-NOTA conjugates of dextrans with molecular weigh tof **(a)** 10 kDa and **(b)** 70 kDa. Biodistribution was measured in diabetic C57Bl/6J mice bearing two full thickness wounds on different parts of the body, 3 days post-wounding. Injection was only in wound 1 and was measured by ex vivo gamma well counting at either 6 hr or 24 hr after injection.

Results: During the award period, we shifted focus from Coxibs to a novel class of anti-inflammatory agents targeting the epigenetically targeted histone demethylase JMJD3. The Gallagher lab identified JMJD3 activity in Mφ-mediated inflammation in tissue repair and its pathologic role in sustaining inflammation in diabetic wounds, so we theorized that cell-specific targeting of JMJD3 would be a viable therapeutic target. D70 was linked with the JMJD3 covalent inhibitor, GSK-J1 (**Fig. 3A**) Following wounding of DIO mice, D70-GSK-J1 was subcutaneously injected (1 mg/kg) into the wounds of the mice daily for 7 days. Wound healing, compared to that of the placebo-treated mice and the *DIO Jmjd3$^{f/f}$Lyz2^{Cre+}* mice (phenotypic control), was monitored and analyzed by ImageJ software and histology. We observed that Mφ-specific inhibition of JMJD3 resulted in significantly improved wound healing in the D70-GSK-J1-treated group and was most pronounced in the later days of wound healing. This period is consistent with the days of highest *Jmjd3* and *Tmem173* expression in diabetic wound Mφs. For comparison, the *DIO Jmjd3$^{f/f}$Lyz2^{Cre+}* mice exhibited improved wound healing similar to the targeted drug-treated cohort. Histologically, wounds harvested on Day 5 of D70-GSK-J1treatment had increased epithelialization compared to the placebo controls, signifying advancement through the normal stages of tissue repair in the treated wounds (**Fig. 3B**). To confirm that the observed effects were mediated by *Jmjd3* inhibition in Mφs, we isolated wound Mφs (CD3$^-$/CD19$^-$/NK1.1$^-$/Ly6G$^-$/CD11b$^+$) from the D70-GSK-J1-treated mice and their controls on Day 5 after wounding and analyzed them. These assays revealed significantly decreased *Tmem173*, *Il1b* and *Tnfa* expression in the wound Mφs from treated wounds compared to the placebo-treated wound Mφs (**Fig. 3C**). Taken together, these data suggest that Mφ-specific targeting of JMJD3 in diabetic wounds ameliorates persistent inflammation resulting from the NFκB and STING pathways and results in improved diabetic wound repair, making this a viable therapeutic strategy. We observed no effects on off-target tissue.

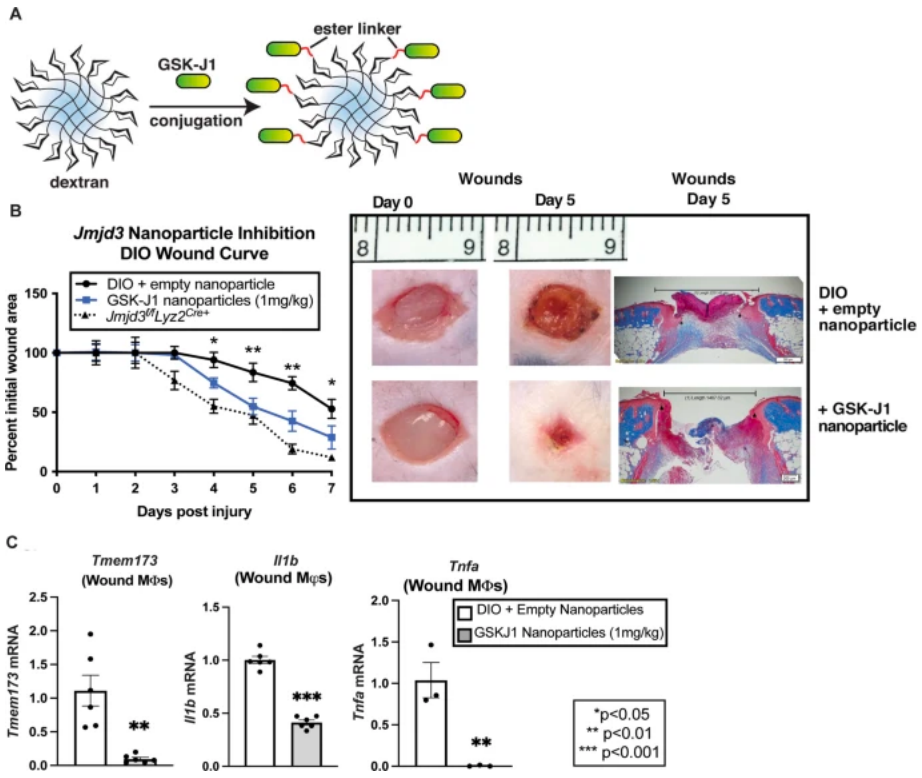

Fig. 3. Anti-inflammatory Mφ-specific therapy improves diabetic tissue repair. **(A)** Schematic of Mφ specific, GSK-J1-laden, dextran core nanoparticles. **(B)** Wound healing curve for DIO mice wounded with a 6 mm punch biopsy, and wounds were injected daily starting on Day 1 post-injury with nanoparticles containing either a selective JMJD3 inhibitor (GSK-J1; 1 mg/kg) or dextrose control. DIO mice deficient in myeloid JMJD3 production (*Jmjd3$^{f/f}$Lyz2^{Cre+}*) were included as a control. Wound area was measured daily with ImageJ software throughout the wound healing course (N = 5/group, repeated twice). Representative wound images at ×2 magnification on Day 0 and Day 5 are shown. Wounds were harvested on Day 5, paraffin embedded, and stained with Masson's trichrome stain (N = 5–6 mice/group). The black bar above the wound represents the entire wound distance, the arrowheads represent the epithelial tongue edges, and the asterisk (*) represents wound debris. The scale bar represents 200 μm. **(C)** *Tmem173*, *Il1b* and *Tnfa* expression in DIO wound Mφs (CD3$^-$/CD19$^-$/NK1.1$^-$/Ly6G$^-$/CD11b$^+$) harvested on Day 5 from wounds treated with and without GSK-J1 nanoparticles (N = 3–4/group, pooled, repeated in triplicate). *p < 0.05, **p < 0.01. Data are presented as the mean ± SEM. Data were first analyzed for normal distribution, and if data passed the normality test, a two-tailed Student's t-test was used

3. Publications:

Audu CO, Melvin WJ, Joshi AD, Wolf SJ, Moon JY, Davis FM, Barrett EC, Mangum KD, Deng H, Xing W, Wasikowski R, Tsoi LC, Sharma SB, Bauer TM, Shadiow J, Corriere MA, Obi AT, Kunkel SL, Levi BS, Moore BB, Gudjonsson JE, Smith AM, Gallagher KA. Macrophage-specific inhibition of the histone demethylase JMJD3 decreases STING and pathologic inflammation in diabetic wound repair. *Cell and Molecular Immunology*. 19: 1251-1262 (2022). https://doi.org/10.1038/s41423-022-00919-5